bioRxiv preprint doi: https://doi.org/10.1101/2021.05.13.444049; this version posted May 14, 2021. The copyright holder for this preprint (which was not certified by peer review) is the author/funder, who has granted bioRxiv a license to display the preprint in perpetuity. It is made available under aCC-BY-NC-ND 4.0 International license.

1 # RNA-seq and differential expression analysis of the duck
2 # transcriptome: The effect of short-term cage-rearing

3 Biao Chen[*,†], Wenjie Fang[*,†], Yankai Li[*,†], Ting Xiong[*,†], Mingfang Zhou[*,†], Lei
4 Wan[*,†], Qiuhong Liu[*,†], Wenyan Zhang[*], Xiaolong Hu[*,†], Huirong Mao[*,†], Sanfeng
5 Liu[*,†,1]

6 *College of Animal Science and Technology, Jiangxi Agricultural University,
7 Nanchang 330045, Jiangxi, China; chenbiao@jxau.edu.cn (B.C.);
8 F461962829@163.com (W.F.); L1457172529@163.com (Y.L.); xt970123@163.com
9 (T.X.); bighawkin@sina.com (M.Z.); gaosan0211@163.com (L.W.);
10 liuqiuhong157@163.com (Q.L.); zhangwenyan9911@163.com (W.Z.);
11 huxiaolong@jxau.edu.cn (X.H.); huirongmjxau@126.com (H.M.);

12 †Institute of Poultry Science, Jiangxi Agricultural University, Nanchang 330045,
13 Jiangxi, China;

14

15 **Data Availability Statement:** All sequencing data were uploaded to in the Gene
16 Expression Omnibus (GEO) with accession number GSE173134
17 (https://www.ncbi.nlm.nih.gov/geo/query/acc.cgi?acc=GSE173134).

18

bioRxiv preprint doi: https://doi.org/10.1101/2021.05.13.444049; this version posted May 14, 2021. The copyright holder for this preprint (which was not certified by peer review) is the author/funder, who has granted bioRxiv a license to display the preprint in perpetuity. It is made available under aCC-BY-NC-ND 4.0 International license.

19 **RUNNING TITLE: Caging-induced duck gene regulation**

20

21 **Keywords:** Duck; Transcriptome regulation; Cage-rearing system; Floor-water
22 combination system

23

24 1 Correspondence: College of Animal Science and Technology, Jiangxi Agricultural
25 University, Nanchang 330045, Jiangxi, China; lsf3318@jxau.edu.cn, Tel.:
26 +86-791-83813503 (S.L.)

27

bioRxiv preprint doi: https://doi.org/10.1101/2021.05.13.444049; this version posted May 14, 2021. The copyright holder for this preprint (which was not certified by peer review) is the author/funder, who has granted bioRxiv a license to display the preprint in perpetuity. It is made available under aCC-BY-NC-ND 4.0 International license.

28 **Abstract:** Ducks are an important source of meat and egg products for human beings.
29 In China, duck breeding has gradually changed from the traditional floor-water
30 combination system to multilayer cage breeding. Therefore, the present study
31 collected the hypothalamus and pituitary of 113-day-old ducks after being caged for 3
32 days, in order to investigate the effect of cage-rearing on the birds. In addition, the
33 same tissues (hypothalamus and pituitary) were collected from ducks raised in the
34 floor-water combination system, for comparison. Thereafter, the transcriptomes were
35 sequenced and the expression level of genes were compared. The results of
36 sequencing analysis showed that a total of 506 and 342 genes were differentially
37 expressed in the hypothalamus and pituitary, respectively. Additionally, the
38 differentially expressed genes were mainly enriched in signaling pathways involved in
39 processing environmental information, including ECM-receptor interaction,
40 neuroactive ligand-receptor interaction and focal adhesion. The findings also showed
41 that there was a change in the alternative splicing of genes when ducks were
42 transferred into the cage rearing system. However, there was no difference in the
43 expression of some genes although there was a change in the expression of the
44 isoforms of these genes. The findings herein can therefore help in understanding the
45 mechanisms underlying the effect of caging on waterfowl. The results also highlight
46 the gene regulatory networks involved in animal responses to acute stress.

47 ## Introduction

48 The consumption of poultry products across the globe has increased over the years.

bioRxiv preprint doi: https://doi.org/10.1101/2021.05.13.444049; this version posted May 14, 2021. The copyright holder for this preprint (which was not certified by peer review) is the author/funder, who has granted bioRxiv a license to display the preprint in perpetuity. It is made available under aCC-BY-NC-ND 4.0 International license.

49 Notably, China is the world's largest producer and consumer of duck products
50 (http://www.fao.org/faostat/en/#data/QA/visualize). In addition, the floor-water
51 combination system is the conventional method of rearing ducks in China (Figure 1A).
52 This feeding system is highly dependent on the water area. However, the conventional
53 floor-water combination system of rearing ducks has many shortcomings. Such
54 include poor utilization of water resources, serious pollution to the water environment
55 which limits large scale production as well as disease control and low economic
56 benefits. Therefore, it is necessary to adopt an environmentally friendly breeding
57 model for ducks. Over the recent years, the cage rearing system has developed rapidly
58 in duck production because it is environmentally friendly and has several economic
59 benefits(BAI *et al.* 2020). Moreover, the cage rearing system for ducks is
60 characterized by high stocking densities, clean egg surfaces and high uniformity of
61 waterfowl (Figure 1 B). However, the system has not been explored extensively.
62 Compared to chicken husbandry, such factors as body size, dabbling, fecal ejection
63 and other habits, complicate the design, manufacture and production of ducks.
64 Additionally, the acute and chronic stress caused by cage rearing are also crucial
65 issues that need to be addressed by duck producers(ZHANG *et al.* 2019). In the cage
66 rearing system, the high-density husbandry causes spatial stress to the ducks.
67 Moreover, high density stocking increases the concentration of hydrogen sulfide,
68 ammonia and other harmful gases in duck cages, which are detrimental to the growth
69 and reproduction of the birds(SHEPHERD *et al.* 2015; ZHAO *et al.* 2016). In addition,

bioRxiv preprint doi: https://doi.org/10.1101/2021.05.13.444049; this version posted May 14, 2021. The copyright holder for this preprint (which was not certified by peer review) is the author/funder, who has granted bioRxiv a license to display the preprint in perpetuity. It is made available under aCC-BY-NC-ND 4.0 International license.

70 the air velocity and relative humidity in the cage rearing system are quite different
71 from those in the floor-water combination system(EN-CAI *et al.* 2020). These
72 environmental changes therefore trigger stress responses and adaptive changes in
73 ducks.

74 Moreover, ducks experience several changes in their living environment when they
75 are initially transferred into cages, resulting to stress responses in their bodies(ZHANG
76 *et al.* 2019). Stress refers to a non-specific response of the body to external stimuli
77 and can be classified as either acute or chronic stress. Notably, the body mainly
78 responds to stress through the Hypothalamus-pituitary-adrenal axis
79 (HPA)(NICOLAIDES *et al.* 2014; OYOLA and HANDA 2017). After the center of the
80 brain receives external stimulation, the information is transmitted to the hypothalamus.
81 The hormone secreted from the hypothalamus then stimulates the pituitary gland to
82 secrete the adrenocorticotropic hormone, putting the body in a state of full
83 mobilization. The body in turn experiences an increase in heart rate, blood pressure,
84 body temperature, muscle tension, metabolic level and other significant changes, so as
85 to enhance body activity and cope with emergencies(MUNAKATA 2018; NICOLAIDES
86 *et al.* 2014).

87 Therefore, it is important for duck producers and researchers to analyze the internal
88 mechanism of high-density cage-rearing stress in egg laying ducks in order to develop
89 methods for stress alleviation and improve the reproductive performance of
90 cage-reared waterfowl. Consequently, the current study compared the transcriptomes

bioRxiv preprint doi: https://doi.org/10.1101/2021.05.13.444049; this version posted May 14, 2021. The copyright holder for this preprint (which was not certified by peer review) is the author/funder, who has granted bioRxiv a license to display the preprint in perpetuity. It is made available under aCC-BY-NC-ND 4.0 International license.

91 of the hypothalami and pituitary from ducks reared in the two husbandry systems (the
92 traditional floor-water combination and cage-rearing systems). In addition, the study
93 investigated the candidate genes and signaling pathways involved in cage-rearing
94 stress. By exploring the regulatory mechanism of cage-rearing stress in egg laying
95 ducks, this study provides a fundamental basis for establishing new methods of
96 solving caging related stress in waterfowl. This in turn promotes the development and
97 popularization of the waterfowl caging technology and also provides more insights on
98 the molecular mechanism of the interaction between genes and the environment.

99 ## Materials and Methods

100 ### Ethical statement

101 All the animal experiments in this study were conducted according to the ethical
102 standards of the Jiangxi Agricultural University (JXAULL-2017002). The ducks were
103 sacrificed painlessly.

104 ### Animals and management

105 A total of 30 female Shan Ma ducks (*Anas platyrhynchos*) were purchased from the
106 Jiangxi Tianyun duck breeding farm (Nanchang, Jiangxi) and reared in the Anyi duck
107 farm of Jiangxi. All the ducks were then transported to the Anyi duck farm after
108 reaching the age of 100 days, then raised in the floor-water combination system
109 (Figure 1A). At the age of 110 days, fifteen ducks were randomly selected and
110 transferred into three cages (100 × 45 × 50 cm, Figure 1B) while the others were
111 retained in the floor-water feeding system. All the ducks were kept at room

bioRxiv preprint doi: https://doi.org/10.1101/2021.05.13.444049; this version posted May 14, 2021. The copyright holder for this preprint (which was not certified by peer review) is the author/funder, who has granted bioRxiv a license to display the preprint in perpetuity. It is made available under aCC-BY-NC-ND 4.0 International license.

112 temperature and fed with the commercial diet produced by the Nanchang Huada
113 Group (Nanchang, Jiangxi, China). Additionally, the ducks raised in the floor-water
114 system (FW group) received natural illumination while the 15 ducks raised in cages
115 (C group) were subjected to a standard regimen involving 16 h of light. All the ducks
116 remained in good health in the entire duration of the experiment.
117

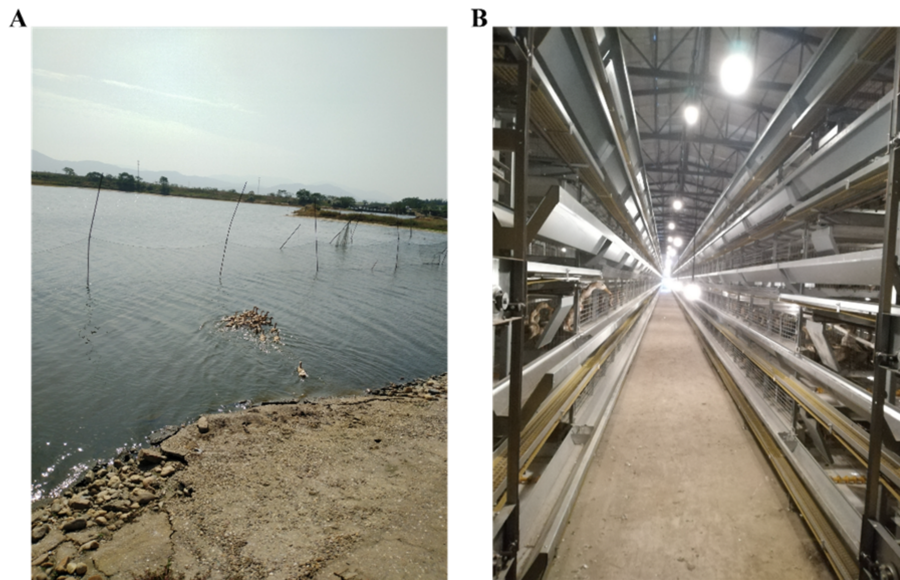

118

119 **Figure 1** The two feeding systems used in the current study. (**A**) The conventional floor-water
120 combination system for ducks. (**B**) The multilayer cage-rearing system for ducks.
121

122 **Sample collection and RNA extraction**

123 After 3 days of changing the rearing system, all ducks in the FW and C groups were
124 sacrificed. The hypothalami and pituitaries were then sampled using scissors and
125 tweezers, snap-frozen with liquid nitrogen then kept in -80 °C. Thereafter, total RNA
126 was extracted using the TRIzol reagent (Invitrogen, CA, USA), according to the

bioRxiv preprint doi: https://doi.org/10.1101/2021.05.13.444049; this version posted May 14, 2021. The copyright holder for this preprint (which was not certified by peer review) is the author/funder, who has granted bioRxiv a license to display the preprint in perpetuity. It is made available under aCC-BY-NC-ND 4.0 International license.

127 manufacturer's instructions. In addition, the purity and quantity of RNA were
128 evaluated using NanoDrop ND-1000 (NanoDrop, DE, USA). Moreover, RNA
129 integrity was assessed through electrophoresis in denaturing agarose gel and
130 Bioanalyzer 2100 (Agilent, CA, USA) with a RIN number >7.0.

131 **RNA library construction and sequencing**

132 After confirming the quality of RNA, four samples from each group were selected to
133 construct the RNA library. Notably, Poly (A) RNA was obtained from 2 μg of total
134 RNA using the Dynabeads Oligo (dT)25-61005 Kit (Thermo Fisher, CA, USA), with
135 two rounds of purification. Thereafter, the poly (A) product was broken into pieces at
136 94 °C for 5-7 min using the Magnesium RNA Fragmentation Module (NEB, MA,
137 USA). The RNA fragments were then reverse-transcribed using the SuperScript™ II
138 Reverse Transcriptase (Invitrogen) in order to construct the cDNA library. Moreover,
139 the U-labeled second-stranded DNAs were synthesized using the cDNA library
140 obtained from the previous step, *Escherichia coli* (*E.coli*) DNA polymerase I (NEB),
141 RNase H (NEB) and a dUTP solution (Thermo Fisher). After adaptor ligation, the
142 product was treated with the heat-labile UDG enzyme. Finally, the products were
143 amplified through PCR in the following steps: 95 °C for 3 min; 8 cycles of 98 °C for
144 15 sec, 60 °C for 15 sec and 72 °C for 30 sec then a final step of 72°C for 5 min.
145 Thereafter, the PCR products were submitted for 2 × 150 bp paired-end sequencing
146 (PE150) on the Illumina Novaseq™ 6000 platform (LC-Bio Technology CO., Ltd.,
147 Hangzhou, China), following the manufacturer’s instructions.

bioRxiv preprint doi: https://doi.org/10.1101/2021.05.13.444049; this version posted May 14, 2021. The copyright holder for this preprint (which was not certified by peer review) is the author/funder, who has granted bioRxiv a license to display the preprint in perpetuity. It is made available under aCC-BY-NC-ND 4.0 International license.

148 **Bioinformatics analysis of RNA-Seq data**

149 Cutadapt (https://cutadapt.readthedocs.io/en/stable/) was used to remove the reads
150 containing adaptors and low-quality bases in order to ease analysis in the next step.
151 Thereafter, HISAT2 (https://daehwankimlab.github.io/hisat2/, version: 2-2.0.4) was
152 used to map the reads to the duck genome
153 (https://www.ncbi.nlm.nih.gov/genome/2793?genome_assembly_id=426073). The
154 mapped reads in each sample were then assembled using StringTie
155 (http://ccb.jhu.edu/software/stringtie/, version: stringtie-1.3.4d), with default
156 parameters. Afterwards, a comprehensive transcriptome was reconstructed with the
157 mapped reads from all the samples, using the gffcompare software
158 (http://ccb.jhu.edu/software/stringtie/gffcompare.shtml, version: gffcompare-0.9.8). In
159 addition, StringTie and ballgown
160 (http://www.bioconductor.org/packages/release/bioc/html/ballgown.html) were
161 employed to evaluate the expression levels of all the transcripts and genes in each
162 sample by calculating the fragments per kilobase of exon per million mapped
163 fragments (FPKM). Moreover, the differentially expressed mRNAs (DEGs) and
164 differentially expressed transcripts (DETs) were selected based on the following
165 criteria; $|\log2 \text{ fold change}| \geq 1$ and $p \leq 0.05$ using the DESeq2 package in R
166 (http://www.bioconductor.org/packages/release/bioc/html/DESeq2.html). After
167 obtaining the list of DEGs, enrichment analyses, including Gene Ontology (GO) and
168 Kyoto Encyclopedia of Genes and Genomes (KEGG), were performed using the

bioRxiv preprint doi: https://doi.org/10.1101/2021.05.13.444049; this version posted May 14, 2021. The copyright holder for this preprint (which was not certified by peer review) is the author/funder, who has granted bioRxiv a license to display the preprint in perpetuity. It is made available under aCC-BY-NC-ND 4.0 International license.

169 DAVID 6.7 functional annotation tool (http://david.abcc.ncifcrf.gov/), in order to
170 assess the potential processes associated with acute stress during cage-rearing.

171 **Complementary DNA (cDNA) synthesis and qPCR**

172 The cDNA libraries were constructed from total RNA using the Monad MonScript™
173 All-in-One Kit with DNase (Biopro, Shanghai, China) and reverse-transcription was
174 conducted following the manufacturer's instructions. Thereafter, the cDNA libraries
175 were diluted in nuclease-free water at a ratio of 1:4 for qPCR. The expression levels
176 of candidate genes were then quantified through qPCR using the 2 × T5 Fast qPCR
177 Mix (TsingKe, Beijing, China) on an ABI QuantStudio 5 system (Thermo Fisher,
178 Waltham, MA, USA). The *GAPDH* gene was used as the internal reference and the
179 final volume of the qPCR reaction was 20 µl. The following conditions were used for
180 qPCR: 95 °C for 3 min; 40 cycles of 95 °C for 10 s, Tm for 1 min and collection of
181 fluorescence at 65 – 95 °C. Additionally, each sample was analyzed in triplicate and
182 the relative expression levels were calculated according to the comparative $2^{-\Delta\Delta Ct}$
183 method. The primer pairs used in this study were designed using Primer Premier
184 Version 5 (Premier Biosoft, CA, USA). Information on the qPCR primers for the
185 candidate genes and *GAPDH* is shown in Table 1.

186 **Statistical Analysis**

187 The qPCR results were presented as the mean ± standard error of the mean (S.E.M.).
188 In addition, the Students two-tailed t-test was used for statistical analysis. The level of
189 significance was set at * ($p < 0.05$), ** ($p < 0.01$) and *** ($p < 0.001$).

bioRxiv preprint doi: https://doi.org/10.1101/2021.05.13.444049; this version posted May 14, 2021. The copyright holder for this preprint (which was not certified by peer review) is the author/funder, who has granted bioRxiv a license to display the preprint in perpetuity. It is made available under aCC-BY-NC-ND 4.0 International license.

190 **Data Availability**

191 Supplemental files available at FigShare. Figure S1: The distribution of mapping
192 region on reference genome, Figure S2: Differential expression analysis of all
193 transcripts, Table S1: Overview of quality of sequencing data, Table S2: All genes
194 detected in current project, Table S3: All the DEGs in the C_H vs. FW_H and C_P vs.
195 FW_P comparisons , Table S4: All information of DETs, Table S5: List of GO
196 enrichment with all DEGs in C_H vs. FW_H, Table S6: List of GO enrichment with
197 all DEGs in C_P vs. FW_P, Table S7: List of KEGG pathways with all DEGs in C_H
198 vs. FW_H, Table S8: List of KEGG pathways with all DEGs in C_P vs. FW_P, Table
199 S9: List of the alternative splicing genes in C_H vs. FW_H and C_P vs. FW_P
200 comparisons. All sequencing data were uploaded to in the Gene Expression Omnibus
201 (GEO) with accession number GSE173134
202 (https://www.ncbi.nlm.nih.gov/geo/query/acc.cgi?acc=GSE173134).

203 **Results**

204 **Summary of Transcriptome Data**

205 In this study, a mean of 48,143,316 validated reads were obtained from each sample.
206 In addition, the proportion of validated reads whose base recognition accuracy met the
207 Q30 standard (the error rate was less than 1%) was greater than 97.6% (Table S1).
208 All the clean reads were then mapped to the duck genome (*Anas platyrhynchos*). The
209 results in Table 2 show that the proportion of mapped validated reads was not less
210 than 74.88% in all the sixteen samples, the percentage of unique mapped reads ranged

bioRxiv preprint doi: https://doi.org/10.1101/2021.05.13.444049; this version posted May 14, 2021. The copyright holder for this preprint (which was not certified by peer review) is the author/funder, who has granted bioRxiv a license to display the preprint in perpetuity. It is made available under aCC-BY-NC-ND 4.0 International license.

211 from 40.44% to 58.50% and the proportion of Pair-end (PE) mapped reads ranged
212 from 53.95% to 78.60%. Moreover, sequence alignment showed that more than 88.3%
213 of the validated reads mapped to the exonic region of each sample (Figure S1).
214 Furthermore, a total of 24,263 genes were detected in all the samples, including
215 annotated and novel genes (Table S2). Out of all the genes, the Growth Hormone 1
216 (GH1) gene had the highest level of expression after *GAPDH,* in both the
217 hypothalamus and pituitary (Table S2).

218 **Identification of differentially expressed genes (DEGs)**

219 In order to investigate the potential candidate genes and pathways associated with
220 cage-rearing stress, the study performed differential expression analysis, where $|\log2$
221 $\text{fold change}| \geq 1$ and $\text{p-value} \leq 0.05$ were selected as the screening criteria (Figure 2A
222 and B). As a result, a total of 506 DEGs were obtained in the hypothalamus (C_H vs.
223 FW_H) out of which 445 were up-regulated and 61 were down-regulated (Figure 2C).
224 On the other hand, a total of 342 DEGs, including 75 up-regulated and 267
225 down-regulated genes, were obtained in the pituitary (C_P vs. FW_P, Figure 2C). All
226 the DEGs are listed in Table S3. Notably, the top 3 most highly expressed genes with
227 the smallest q-values in the hypothalamus (C_H vs. FW_H) were *GH1*, Transthyretin
228 (TTR) and Chromogranin A (CHGA). On the other hand, the Nuclear Receptor
229 Subfamily 4 Group A Member 1 (NR4A1), Transgelin (TAGLN) and Superoxide
230 Dismutase 3 (SOD3) were the top 3 most highly expressed genes in the pituitary (C_P
231 vs. FW_P). Additionally, the study assessed the Differentially Expressed Transcripts

bioRxiv preprint doi: https://doi.org/10.1101/2021.05.13.444049; this version posted May 14, 2021. The copyright holder for this preprint (which was not certified by peer review) is the author/funder, who has granted bioRxiv a license to display the preprint in perpetuity. It is made available under aCC-BY-NC-ND 4.0 International license.

232 (DETs) using the same criteria as those for DEGs (Figure S2A and B). A total of 1019
233 DETs were detected in the hypothalamus (C_H vs. FW_H), out of which 612 were
234 up-regulated and 407 were down-regulated (Figure 2D). Moreover, a total of 916
235 DETs were obtained in the pituitary (C_P vs. FW_P), out of which 438 were
236 up-regulated and 478 were down-regulated (Figure 2D). All the information on DETs
237 is shown in Table S4. The study then performed clustering analysis on the top 50
238 DEGs (50 DEGs with the smallest q-values) in each comparison and the findings
239 were presented as the normalized $\log_2$ FPKM. The results of cluster analysis showed
240 that the upregulated and downregulated genes were quite distinct in each comparison
241 (Figure 2E and F). Clustering analysis was also performed on the top 100 DETs in
242 each comparison. Similar results to those of clustering analysis on DEGs were
243 obtained. However, the number of up- and down-regulated DETs were almost similar,
244 contrary to that of DEGs (Figure S2C and D).
245

bioRxiv preprint doi: https://doi.org/10.1101/2021.05.13.444049; this version posted May 14, 2021. The copyright holder for this preprint (which was not certified by peer review) is the author/funder, who has granted bioRxiv a license to display the preprint in perpetuity. It is made available under aCC-BY-NC-ND 4.0 International license.

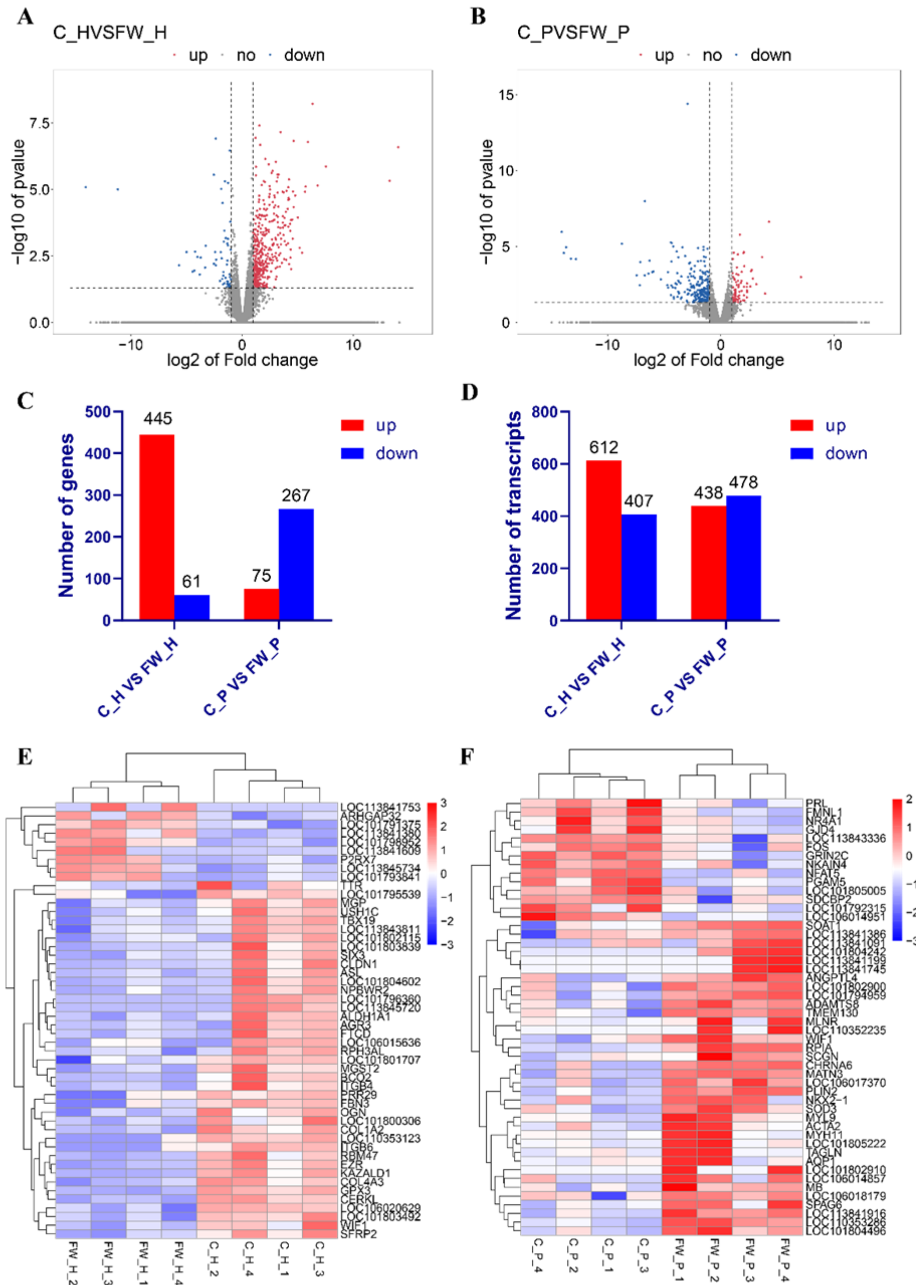

246

247 **Figure 2** Differential expression analysis of the C and FW groups. (**A, B**) Volcano charts of the genes

248 expressed in the C_H vs. FW_H and C_P vs. FW_P comparisons, respectively. Red dots represent

249 up-regulated DEGs, blue dots depict down-regulated DEGs and gray dots indicate no difference in

250 expression. (**C**) The numbers of up-regulated and down-regulated DEGs in the C_H vs. FW_H and

251 C_P vs. FW_P comparisons. (**D**) The numbers of up-regulated and down-regulated DETs in the C_H vs.

bioRxiv preprint doi: https://doi.org/10.1101/2021.05.13.444049; this version posted May 14, 2021. The copyright holder for this preprint (which was not certified by peer review) is the author/funder, who has granted bioRxiv a license to display the preprint in perpetuity. It is made available under aCC-BY-NC-ND 4.0 International license.

252 FW_H and C_P vs. FW_P comparisons. (**E, F**) Heat maps of DEGs in the C_H vs. FW_H and C_P vs.
253 FW_P comparisons, respectively. The top 50 DEGs are shown in each comparison.
254

255 **Enrichment analysis of DEGs**

256 The study then conducted GO enrichment analysis on the DEGs. All the GO terms
257 were classified into three sections, namely; Biological Process (BP), Cellular
258 Component (CC) and Molecular Function (MF), based on functional annotation. The
259 results of GO functional enrichment analysis showed that a total of 378 GO terms
260 were significantly enriched in the C_H vs. FW_H comparison, out of which 259 were
261 enriched in biological process, 50 in cellular component and 68 in molecular function
262 ($p < 0.05$, Table S5). Notably, the GO terms that might have been associated with
263 acute stress were enriched in the glucocorticoid biosynthetic process, thyroid hormone
264 transport, development of the adrenal gland, positive regulation of cortisol secretion,
265 activity of the corticotropin releasing hormone, the steroid hormone mediated
266 signaling pathway, steroid hormone receptor activity and regulation of response to
267 oxidative stress (Figure 3A, Table S5). Additionally, the significant enrichment of
268 sensory perception of the light stimulus (GO:0050953), suggested that the light in the
269 cage-rearing system elicited a different response from to that in the floor-water
270 combination system. On the other hand, a total of 389 GO terms were significantly
271 enriched in the C_P vs. FW_P comparison, including 290 biological process terms, 34
272 cellular component terms and 65 molecular function terms ($p < 0.05$, Table S6).

bioRxiv preprint doi: https://doi.org/10.1101/2021.05.13.444049; this version posted May 14, 2021. The copyright holder for this preprint (which was not certified by peer review) is the author/funder, who has granted bioRxiv a license to display the preprint in perpetuity. It is made available under aCC-BY-NC-ND 4.0 International license.

273 Interestingly, cellular response to the estradiol stimulus, regulation of dopamine
274 secretion, negative regulation of blood pressure, regulation of inflammatory response,
275 detection of oxidative stress and other stress-related terms were among the most
276 significantly enriched GO terms (Figure 3B, Table S6). It is also noteworthy that light
277 associated terms (response to absence of light and retina homeostasis) and
278 reproduction related terms (developmental process involved in reproduction and
279 regulation of female receptivity) were also markedly enriched (Table S6).
280 Furthermore, KEGG pathway analysis was performed on all the DEGs. Results from
281 the C_H vs. FW_H comparison showed that a total of 19 pathways were significantly
282 enriched ($p < 0.1$, Figure 3C). The significantly enriched pathways ($p < 0.05$) are
283 shown in Table 3. Notably, long-term depression, adrenergic signaling in
284 cardiomyocytes and endocrine and other factor-regulated calcium reabsorption were
285 associated with stress (Table S7). Additionally, ECM-receptor interaction, neuroactive
286 ligand-receptor interaction and focal adhesion, were associated with external signal
287 transduction and signaling-molecule interaction. On the other hand, the DEGs in the
288 C_P vs. FW_P comparison were significantly enriched in 9 pathways ($p < 0.1$, Figure
289 3D). Interestingly, the top 3 markedly enriched pathways, i.e., ECM-receptor
290 interaction, focal adhesion and neuroactive ligand-receptor interaction, were also
291 among the top KEGG pathways identified in the hypothalamus. Moreover, pathways
292 related to biosynthesis and substance metabolism, including pantothenate and CoA
293 biosynthesis, nitrogen metabolism and glutathione metabolism, were enriched in the

bioRxiv preprint doi: https://doi.org/10.1101/2021.05.13.444049; this version posted May 14, 2021. The copyright holder for this preprint (which was not certified by peer review) is the author/funder, who has granted bioRxiv a license to display the preprint in perpetuity. It is made available under aCC-BY-NC-ND 4.0 International license.

294 C_P vs. FW_P comparison (Table S8). In addition, a total of 13 DEGs were enriched
295 in ECM-receptor interaction pathways, including the Collagen Type VI Alpha 1 Chain
296 (COL6A1), Chondroadherin (CHAD), Thrombospondin 2 (THBS2), Syndecan 1
297 (SDC1), the Integrin Binding Sialoprotein (IBSP), Tenascin R (TNR), the SLIT and
298 NTRK Like Family Member 1 (SLITRK1), the Von Willebrand Factor (VWF), the
299 Laminin Subunit Alpha 4 (LAMA4), Tenascin C (TNC), the Integrin Subunit Alpha
300 11 (ITGA11), Glycoprotein Ib Platelet Subunit Alpha (GP1BA) and *COL2A1* (Table
301 4). Notably, the recurrence of *COL6A2*, *COL1A2*, *LAMA5*, *COL6A1*, *COL2A1* and
302 *LAMA4* (members of the COL and LAMA families) in both comparisons, suggested
303 that they might be associated with caging related stress in ducks.
304

305

306 **Figure 3** Enrichment analysis of DEGs. (**A, B**) GO classification of the DEGs in C_H vs. FW_H and

bioRxiv preprint doi: https://doi.org/10.1101/2021.05.13.444049; this version posted May 14, 2021. The copyright holder for this preprint (which was not certified by peer review) is the author/funder, who has granted bioRxiv a license to display the preprint in perpetuity. It is made available under aCC-BY-NC-ND 4.0 International license.

307 C_P vs. FW_P, respectively. The top 20, 15, and 10 GO terms in biological processes, cellular
308 components, and molecular functions, respectively, are shown. (**C, D**) The significantly enriched
309 KEGG signaling pathways (P<0.1) of the DEGs in C_H vs. FW_H and C_P vs. FW_P, respectively.
310

311 **Validation of sequencing data**

312 After conducting enrichment analysis, 5 DEGs were selected from each comparison to
313 validate the sequencing data. Therefore, the study designed the specific qPCR primers
314 for Beta-carotene Oxygenase 2 (BCO2), Matrix Gla Protein (MGP), Loc101791375,
315 Loc106020629 and Corticotropin Releasing Hormone (CRH). The qPCR results
316 showed that the expression trends were consistent with those of the RNA-seq data in
317 the C_H vs. FW_H comparison (Figure 4A). On the other hand, the qPCR-assessed
318 trends in the expression of SOD3, Myosin Light Chain 9 (MYL9), Fos
319 Proto-Oncogene (FOS), Ribose 5-Phosphate Isomerase A (RPIA) and PGAM Family
320 Member 5 (PGAM5) in the C_P vs. FW_P comparison, were consistent with those in
321 the RNA-seq data (Figure 4B).
322

bioRxiv preprint doi: https://doi.org/10.1101/2021.05.13.444049; this version posted May 14, 2021. The copyright holder for this preprint (which was not certified by peer review) is the author/funder, who has granted bioRxiv a license to display the preprint in perpetuity. It is made available under aCC-BY-NC-ND 4.0 International license.

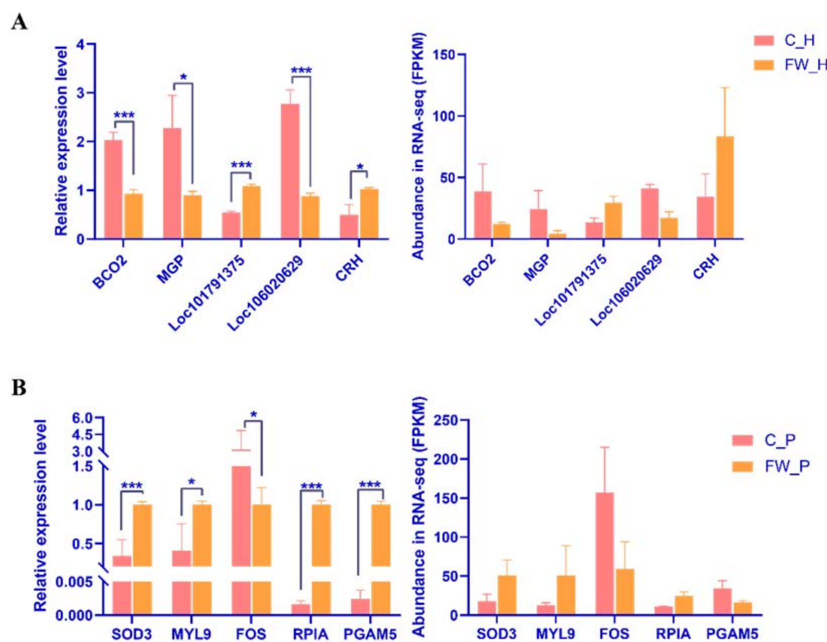

323

324 **Figure 4** qRT-PCR validation of the DEGs. The graphs on the left represent the qPCR results of the

325 selected DEGs in the (**A**) C_H vs. FW_H comparison and (**B**) in the C_P vs. FW_P comparison. On the

326 other hand, the graphs on the right represent the expression level of DEGs in RNA-seq data. The values

327 are presented as the mean ± SEM in all the panels. * $p < 0.05$; ** $p < 0.01$; *** $p < 0.001$.

328

329 **Cage-rearing stress altered RNA splicing**

330 After analyzing the number of differentially expressed transcripts and genes, the

331 results showed that there was a huge difference in the number up-regulated and

332 down-regulated DEGs but little difference between the corresponding up-regulated

333 and down-regulated DETs. Therefore, it was speculated that the parental genes of

334 multiple differentially expressed transcripts were not DEGs. This phenomenon may

335 have occurred because the two differential transcripts from the same parental gene

336 were oppositely regulated or the expression levels of the differential transcripts was

bioRxiv preprint doi: https://doi.org/10.1101/2021.05.13.444049; this version posted May 14, 2021. The copyright holder for this preprint (which was not certified by peer review) is the author/funder, who has granted bioRxiv a license to display the preprint in perpetuity. It is made available under aCC-BY-NC-ND 4.0 International license.

337 lower, which did not significantly affect the expression of the parental gene. In order
338 to verify this hypothesis, the threshold for DETs screening was set at a q-value < 0.05
339 and the sum of FPKM from 8 samples in one comparison was set to be greater than 20.
340 Based on this threshold, a total of 9 DETs were obtained in the C_H vs. FW_H
341 comparison and 8 DETs met the criteria in the pituitary comparison (Table S9).
342 Notably, there was no difference in the expression of the parental genes of these DETs
343 in their respective comparisons although one or more transcripts were differentially
344 expressed. For instance, in the C_P vs. FW_P comparison, the isoform of Isocitrate
345 Dehydrogenase 1 (IDH1), XM_027461485.1, was significantly down-regulated ($q <$
346 0.001) while XM_027461486.1 was up-regulated ($p < 0.05$). However, there was no
347 difference in the expression of IDH1 between the cage-rearing and the floor-water
348 combination groups (Figure 5A). Similarly, XM_027446641.1 (an isoform of the
349 Receptor Accessory Protein 5, REEP5) was significantly down-regulated ($q < 0.05$)
350 while XM_027446638.1 was up-regulated ($p < 0.05$). Nonetheless, there was no
351 difference in the expression of the other two transcripts and the REEP5 gene in the
352 C_P vs. FW_P comparison (Figure 5B). In the hypothalamic comparison, the isoform
353 of the Ribosomal Protein L7a (RPL7A), XM_027470724.1 was significantly
354 down-regulated ($q < 0.001$) while the expression of the other transcript was
355 significantly higher than that of XM_027470724.1, which did not affect the
356 expression level of the gene (Figure 5C). Moreover, qPCR primers for *IDH1*, *REEP5*
357 and the respective DETs were designed to verify the differential expression of the

bioRxiv preprint doi: https://doi.org/10.1101/2021.05.13.444049; this version posted May 14, 2021. The copyright holder for this preprint (which was not certified by peer review) is the author/funder, who has granted bioRxiv a license to display the preprint in perpetuity. It is made available under aCC-BY-NC-ND 4.0 International license.

358 above transcripts. The results were consistent with the sequencing data, indicating that
359 acute cage-rearing stress can change the alternative splicing of some genes (Figure
360 5D).

361

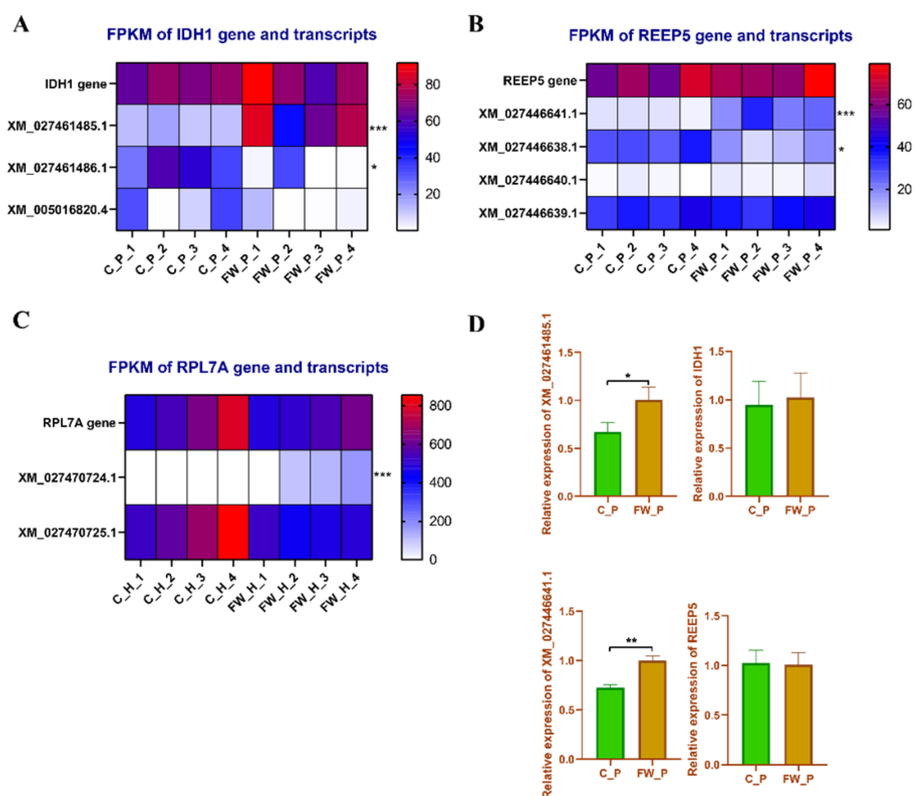

362

363 **Figure 5** Alternative splicing was different between the C and FW groups. (**A, B**) Heat maps of the
364 expression level of *IDH1*, *REEP5* and their isoforms in the C_P vs. FW_P comparison. (**C**) A heat map
365 of the expression of *RPL7A* and its transcripts in the C_H vs. FW_H comparison. (**D**) qPCR validation
366 of *IDH1*, *REEP5* and their isoforms in the C_P vs. FW_P comparison. The values are presented as the
367 mean ± SEM in all the panels. * $p < 0.05$; ** $p < 0.01$; *** $p < 0.001$.

368

bioRxiv preprint doi: https://doi.org/10.1101/2021.05.13.444049; this version posted May 14, 2021. The copyright holder for this preprint (which was not certified by peer review) is the author/funder, who has granted bioRxiv a license to display the preprint in perpetuity. It is made available under aCC-BY-NC-ND 4.0 International license.

369 **Discussion**

370 In China, both food safety and environmental protection are given great emphasis,
371 making farmers to explore more environmentally friendly breeding models for egg
372 laying ducks. In addition, methods of duck breeding have gradually changed from the
373 traditional floor-water combination system to cage breeding(HOU and LIU 2021).
374 Compared to a single cage, multilayer cages have a higher feeding density, which
375 allow for better utilization of space and are more suitable for large-scale feeding as
376 well as management. Moreover, multilayer cage-rearing and floor-water combination
377 breeding are two different feeding methods that can be used as models for studying
378 the interaction between organisms and their environment. Consequently, the current
379 study explored the similarities and differences in gene expression between ducks
380 reared in multilayer cages for three days and those raised in the floor-water
381 combination system. The results therefore provide baseline information for future
382 research on the adaptability of ducks to long-term cage-rearing. The study also has an
383 important economic value and practical significance to the waterfowl industry.

384 Previous research showed that cage-rearing can cause endoplasmic reticulum stress
385 and lead to liver injury in ducks. It was also reported that there was an increase in the
386 expression levels of inflammation-related factors and immune-related genes(ZHANG *et*
387 *al.* 2019). It is noteworthy that changes in the external environment affect the
388 transcriptome of an organism(KRISHNAN *et al.* 2020; WANG *et al.* 2020; XU *et al.*
389 2019). In addition, activation of the HPA axis triggers the hypothalamus to release

bioRxiv preprint doi: https://doi.org/10.1101/2021.05.13.444049; this version posted May 14, 2021. The copyright holder for this preprint (which was not certified by peer review) is the author/funder, who has granted bioRxiv a license to display the preprint in perpetuity. It is made available under aCC-BY-NC-ND 4.0 International license.

390 CRH and Arginine Vasopressin (AVP). CRH stimulates the production and secretion
391 of the Adrenocorticotropic Hormone (ACTH) in the pituitary(DICK and PROVENCAL
392 2018; GUEST and GUEST 2018). The present study caged ducks in the floor-water
393 combination system for three days then assessed the differences between the
394 transcriptomes of ducks reared in cages and those raised in the traditional method.
395 According to previous study, cage-rearing stress gradually subsides after the 4th
396 day(ZHANG *et al.* 2019). Herein, there was a decrease in the expression of the *CRH*
397 gene although there was no significant difference in the expression of the *ACTH* gene
398 (Proopiomelanocortin, POMC). These indicated that the acute stress in ducks had
399 gradually faded at the three days of caging and that they had adapted to their
400 environment. The up-regulation of *CRH* may have been due to the weak response of
401 cage-reared ducks to capture and sampling. On the other hand, ducks raised in the
402 floor-water combination system had a strong response, leading to the down-regulation
403 of *CRH* and no change in *POMC*.

404 In addition, the study conducted differential expression analysis between the two
405 groups and enrichment analysis of DEGs after RNA sequencing. The results of
406 enrichment analysis showed that the DEGs were mainly enriched in processes
407 associated with metabolism and processing of environmental information. Notably,
408 the ECM-receptor interaction, neuroactive ligand-receptor interaction and the focal
409 adhesion signaling pathways were the most significantly enriched pathways in both
410 groups. The ECM-receptor interaction signaling pathway belongs to the

bioRxiv preprint doi: https://doi.org/10.1101/2021.05.13.444049; this version posted May 14, 2021. The copyright holder for this preprint (which was not certified by peer review) is the author/funder, who has granted bioRxiv a license to display the preprint in perpetuity. It is made available under aCC-BY-NC-ND 4.0 International license.

411 environmental information processing subclass
412 (https://www.kegg.jp/dbget-bin/www_bget?pathway+hsa04512). The Extracellular
413 Matrix (ECM) is a three-dimensional acellular structure composed of collagen,
414 Proteoglycan (PG) and glycoprotein. The structure mediates cell-matrix or cell-cell
415 adhesion, signal transduction and cell growth(THEOCHARIS *et al.* 2016). In this study,
416 12 genes including' *COL6A2*, *LAMA2*, *COL1A2* and *ITGB6*, were enriched in the
417 ECM-receptor interaction signaling pathway in the C_H vs. FW_H comparison while
418 13 genes were enriched in the pituitary. Additionally, collagen is an important member
419 of the ECM-receptor interaction signaling pathway(VARGAS *et al.* 2013). The present
420 study showed that several members of the collagen family were significantly
421 differentially expressed. Moreover, it was previously reported that decreasing
422 oxidative stress in cardiomyocytes can reduce the expression of collagen 1 and
423 3(ZHOU *et al.* 2009). In this study, there were significant differences in the expression
424 of *COL6A2*, *COL1A2*, *COL4A4*, COL4A3, *COL4A5*, *COL6A1* and *COL2A1* in the
425 two groups, indicating that they were regulated by stress in the cage environment.
426 Furthermore, the neuroactive ligand-receptor interaction pathway is the aggregation of
427 all receptors and ligands related to intracellular and extracellular signaling pathways
428 in the plasma membrane. The pathway also belongs to the Environmental Information
429 Processing subclass
430 (https://www.kegg.jp/kegg-bin/show_brite?htext=hsa00001.keg&query=hsa04080).
431 Genes in the neuroactive ligand-receptor interaction pathway are associated with

bioRxiv preprint doi: https://doi.org/10.1101/2021.05.13.444049; this version posted May 14, 2021. The copyright holder for this preprint (which was not certified by peer review) is the author/funder, who has granted bioRxiv a license to display the preprint in perpetuity. It is made available under aCC-BY-NC-ND 4.0 International license.

432 stress response, including psychological, electric shock, heat and other forms of
433 stress(KIM *et al.* 2017; LU *et al.* 2020; LUO *et al.* 2015). In this study, 17 and 14 DEGs
434 were enriched in the neuroactive ligand-receptor interaction pathway in the C_H vs.
435 FW_H and C_P vs. FW_P comparisons, respectively.
436 It is also worth noting that animals change the levels of certain proteins in the body in
437 response to external environmental stimuli when they enter into different
438 environments(SAPOLSKY *et al.* 2000). In addition, the body can regulate the
439 expression of some proteins through alternative splicing in order to cope with changes
440 in the external environment(GOPALAKRISHNAN and KUMAR 2020; SINGH *et al.* 2017;
441 TAPIAL *et al.* 2017). Alternative splicing is the process of selecting different
442 combinations of splicing sites on an mRNA precursor in order to produce different
443 isoforms, resulting in different phenotypes due to distinct levels of expression in the
444 same cell(BIRZELE *et al.* 2008). Moreover, previous studies showed that when the
445 body is faced with stress or bacterial infection, it responds by inducing alternative
446 splicing(MARTIN *et al.* 2019; STAIGER and BROWN 2013; SUN 2017). In this study,
447 there were no differences in the expression levels of some genes between the
448 cage-rearing and floor-water system groups. However, the expression of certain
449 isoforms changed significantly. These results therefore showed that the caged
450 environment can regulate the body's response through alternative splicing.
451 Moreover, light affects the feeding, growth and reproductive behavior of birds(LIU *et*
452 *al.* 2020; PITESKY *et al.* 2019; ZAGURI *et al.* 2020). In the cage-rearing system,

bioRxiv preprint doi: https://doi.org/10.1101/2021.05.13.444049; this version posted May 14, 2021. The copyright holder for this preprint (which was not certified by peer review) is the author/funder, who has granted bioRxiv a license to display the preprint in perpetuity. It is made available under aCC-BY-NC-ND 4.0 International license.

453 poultry receive a stable intensity and duration of light. However, the amount of light
454 received by birds in their natural environment is often unstable due to the influence of
455 weather and geographical location(RANI and KUMAR 2014). In this study, the DEGs
456 were enriched in some GO terms related to light perception, including sensory
457 perception of the light stimulus and response to absence of light. This suggested that
458 the different levels of illumination in the cage-rearing and floor-water combination
459 systems affected the growth and development of the ducks.

460 In this study, the hypothalamus and pituitary of ducks in two different rearing systems
461 were collected for transcriptome sequencing. The results showed that there were
462 significant differences in the expression of stress-related genes and pathways. The
463 findings also showed that the cage-rearing system had an effect on the transcriptome
464 of the ducks. Chronic stress has been the focus of most studies on animal production.
465 Therefore, more attention should be paid to the effects of long-term caging on the
466 growth and production performance of ducks. Additionally, multi-omics can be used
467 to explore the mechanisms underlying the effects of cage-rearing on ducks. Moreover,
468 methods can be established to not only mitigate the impact of caging but also enhance
469 the growth and reproductive performance of ducks.

470 **Conclusions**

471 In summary, the present study assessed the differences in the expression of genes
472 between ducks in the cage-rearing and floor-water combination systems. The results
473 showed that there was a significant change in the expression of genes after short-term

bioRxiv preprint doi: https://doi.org/10.1101/2021.05.13.444049; this version posted May 14, 2021. The copyright holder for this preprint (which was not certified by peer review) is the author/funder, who has granted bioRxiv a license to display the preprint in perpetuity. It is made available under aCC-BY-NC-ND 4.0 International license.

474 caging. The findings also revealed that pathways associated with endocrine and
475 environmental information processing were significantly enriched. Notably,
476 ECM-receptor interaction, neuroactive ligand-receptor interaction and focal adhesion
477 were the main signaling pathways enriched in response to short-term caging.
478 Additionally, the caged environment can regulate the body's response through
479 alternative splicing. These results can therefore help in understanding the mechanisms
480 underlying the effect of cage-rearing on the growth and reproduction of waterfowl.
481 The findings also highlight the gene regulatory networks involved in animal responses
482 to acute stress.

483 **Acknowledgments:** This study was support by the Technology System of Modern
484 Agricultural Poultry Industry of Jiangxi Province (JXARS-09), Research and
485 optimization of shell-less hatching method of avian embryos (190223) and Doctoral
486 start-up fund of Jiangxi Agricultural University. The first author thanks Mrs. Jing Liu
487 and Zhuo Chen for their assistance.

488

489 **References**

490 BAI, H., Q. BAO, Y. ZHANG, Q. SONG and B. LIU *et al.*, 2020 Research Note: Effects of the rearing
491 method and stocking density on carcass traits and proximate composition of meat in small-sized meat
492 ducks. Poultry science **99:** 2011-2016.
493 BIRZELE, F., G. CSABA, and R. ZIMMER, 2008 Alternative splicing and protein structure evolution.
494 Nucleic Acids Res **36:** 550-558.
495 DICK, A., and N. PROVENCAL, 2018 Central Neuroepigenetic Regulation of the
496 Hypothalamic-Pituitary-Adrenal Axis. Progress in molecular biology and translational science **158:**
497 105-127.
498 EN-CAI, B., L. YONG, Z. WEI, Y. CHENG-ZHI and Y. JUN-SHU *et al.*, 2020 Mensuration and analysis of
499 environmental parameters in cascading cage-rearing meat duck house with minimum ventilation in the
500 autumn. Jiangsu Journal of Agricultural Science **36:** 648-655.

bioRxiv preprint doi: https://doi.org/10.1101/2021.05.13.444049; this version posted May 14, 2021. The copyright holder for this preprint (which was not certified by peer review) is the author/funder, who has granted bioRxiv a license to display the preprint in perpetuity. It is made available under aCC-BY-NC-ND 4.0 International license.

501 GOPALAKRISHNAN, K., and S. KUMAR, 2020 Whole-Genome Uterine Artery Transcriptome Profiling
502 and Alternative Splicing Analysis in Rat Pregnancy. Int J Mol Sci **21**.
503 GUEST, F. L., and P. C. GUEST, 2018 Developmental Origins of Stress and Psychiatric Disorders, pp.
504 47-58. Springer New York, New York, NY.
505 HOU, S., and L. LIU, 2021 Current status, future development trend and suggestions
506 of waterfowl industry in 2020. Chinese Journal of Animal Science **57:** 235-239.
507 KIM, J. M., K. S. LIM, M. BYUN, K. T. LEE and Y. R. YANG *et al.*, 2017 Identification of the acclimation
508 genes in transcriptomic responses to heat stress of White Pekin duck. Cell Stress Chaperones **22:**
509 787-797.
510 KRISHNAN, J., J. L. PERSONS, R. PEUSS, H. HASSAN and A. KENZIOR *et al.*, 2020 Comparative
511 transcriptome analysis of wild and lab populations of Astyanax mexicanus uncovers differential effects
512 of environment and morphotype on gene expression. J Exp Zool B Mol Dev Evol **334:** 530-539.
513 LIU, G. J., Z. F. CHEN, X. H. ZHAO, M. Y. LI and Z. H. GUO, 2020 Meta-analysis: Supplementary
514 artificial light and goose reproduction. Anim Reprod Sci **214:** 106278.
515 LU, Y., J. YANG, J. SUN, W. LU and J. H. WANG, 2020 mRNA and miRNA profiles in the nucleus
516 accumbens are associated with psychological stress-induced susceptible and resilient mice. Pharmacol
517 Biochem Behav **199:** 173062.
518 LUO, W., M. FANG, H. XU, H. XING and Q. NIE, 2015 Transcriptome comparison in the
519 pituitary-adrenal axis between Beagle and Chinese Field dogs after chronic stress exposure. Anim
520 Genet **46:** 522-534.
521 MARTIN, A. A., N. EVANTAL, I. L. PATOP, O. BARTOK and R. WEISS *et al.*, 2019 Thermosensitive
522 alternative splicing senses and mediates temperature adaptation in Drosophila. Elife **8**.
523 MUNAKATA, M., 2018 Clinical significance of stress-related increase in blood pressure: current
524 evidence in office and out-of-office settings. Hypertension research **41:** 553-569.
525 NICOLAIDES, N. C., E. KYRATZI, A. LAMPROKOSTOPOULOU, G. P. CHROUSOS and E. CHARMANDARI,
526 2014 Stress, the Stress System and the Role of Glucocorticoids. Neuroimmunomodulation **22:** 6-19.
527 OYOLA, M. G., and R. J. HANDA, 2017 Hypothalamic-pituitary-adrenal and
528 hypothalamic-pituitary-gonadal axes: sex differences in regulation of stress responsivity. Stress **20:**
529 476-494.
530 PITESKY, M., A. THORNGREN, and D. NIEMEIER, 2019 Feeding and lighting practices on small-scale
531 extensive pastured poultry commercial farms in the United States. Poult Sci **98:** 785-788.
532 RANI, S., and V. KUMAR, 2014 Photoperiodic regulation of seasonal reproduction in higher vertebrates.
533 Indian J Exp Biol **52:** 413-419.
534 SAPOLSKY, R. M., L. M. ROMERO, and A. U. MUNCK, 2000 How do glucocorticoids influence stress
535 responses? Integrating permissive, suppressive, stimulatory, and preparative actions. Endocr Rev **21:**
536 55-89.
537 SHEPHERD, T. A., Y. ZHAO, H. LI, J. P. STINN and M. D. HAYES *et al.*, 2015 Environmental assessment
538 of three egg production systems — Part II. Ammonia, greenhouse gas, and particulate matter
539 emissions. Poultry science **94:** 534-543.
540 SINGH, P., C. BORGER, H. MORE and C. STURMBAUER, 2017 The Role of Alternative Splicing and
541 Differential Gene Expression in Cichlid Adaptive Radiation. Genome Biol Evol **9:** 2764-2781.
542 STAIGER, D., and J. W. BROWN, 2013 Alternative splicing at the intersection of biological timing,

bioRxiv preprint doi: https://doi.org/10.1101/2021.05.13.444049; this version posted May 14, 2021. The copyright holder for this preprint (which was not certified by peer review) is the author/funder, who has granted bioRxiv a license to display the preprint in perpetuity. It is made available under aCC-BY-NC-ND 4.0 International license.

543 development, and stress responses. Plant Cell **25:** 3640-3656.
544 SUN, H., 2017 Deciphering alternative splicing and nonsense-mediated decay modulate expression in
545 primary lymphoid tissues of birds infected with avian pathogenic E. coli (APEC). BMC Genet **18:** 21.
546 TAPIAL, J., K. HA, T. STERNE-WEILER, A. GOHR and U. BRAUNSCHWEIG *et al.*, 2017 An atlas of
547 alternative splicing profiles and functional associations reveals new regulatory programs and genes that
548 simultaneously express multiple major isoforms. Genome Res **27:** 1759-1768.
549 THEOCHARIS, A. D., S. S. SKANDALIS, C. GIALELI and N. K. KARAMANOS, 2016 Extracellular matrix
550 structure. Adv Drug Deliv Rev **97:** 4-27.
551 VARGAS, J., R. URIBE-ESCAMILLA, and A. ALFARO-RODRIGUEZ, 2013 [Inhibitory proteins of neuritic
552 regeneration in the extracellular matrix: structure, molecular interactions and their functions.
553 Mechanisms of extracellular balance]. Rev Invest Clin **65:** 336-348.
554 WANG, C., Y. CHEN, H. ZHOU, X. LI and Z. TAN, 2020 Adaptation mechanisms of Rhodococcus sp.
555 CNS16 under different temperature gradients: Physiological and transcriptome. Chemosphere (Oxford)
556 **238:** 124571.
557 XU, Z., W. YOU, Y. ZHOU, W. CHEN and Y. WANG *et al.*, 2019 Cold-induced lipid dynamics and
558 transcriptional programs in white adipose tissue. BMC Biol **17:** 74.
559 ZAGURI, S., J. BARTMAN, N. AVITAL-COHEN, L. DISHON and M. GUMULKA *et al.*, 2020 Targeted
560 differential monochromatic lighting improves broiler breeder reproductive performance. Poult Sci **99:**
561 3697-3708.
562 ZHANG, Y., T. GU, Y. TIAN, L. CHEN and G. LI *et al.*, 2019 Effects of cage and floor rearing system on
563 the factors of antioxidant defense and inflammatory injury in laying ducks. BMC Genetics **20**.
564 ZHAO, Y., D. ZHAO, H. MA, K. LIU and A. ATILGAN *et al.*, 2016 Environmental assessment of three egg
565 production systems – Part III: Airborne bacteria concentrations and emissions. Poultry science **95:**
566 1473-1481.
567 ZHOU, S. X., Y. ZHOU, Y. L. ZHANG, J. LEI and J. F. WANG, 2009 Antioxidant probucol attenuates
568 myocardial oxidative stress and collagen expressions in post-myocardial infarction rats. J Cardiovasc
569 Pharmacol **54:** 154-162.

570

571

bioRxiv preprint doi: https://doi.org/10.1101/2021.05.13.444049; this version posted May 14, 2021. The copyright holder for this preprint (which was not certified by peer review) is the author/funder, who has granted bioRxiv a license to display the preprint in perpetuity. It is made available under aCC-BY-NC-ND 4.0 International license.

572 **Table 1** Primer information

Primer names	Sequence (5'-3')	Annealing temperature (°C)	Product size (bp)
qBCO2-F	CACGCTTCGATACGCCAAAG	60	90
qBCO2-R	AGGTGTTCTCACTGCTGACG		
qMGP-F	TCTGTGGGAAGAGAGCGAGA	60	141
qMGP-R	GCTCTCGTGGGACTCATAGC		
qLoc101791375-F	TCCTGTTGCTTGCTCGTAGG	60	125
qLoc101791375-R	GTGAGATGGTTGACGCAGGA		
qLoc106020629-F	AGTGGAGCCAAACCCACTTT	60	111
qLoc106020629-R	CAGTAAAGCCAGCACGCAAG		
qCRH-F	CCTCCGCCACCAACTTTT	60	250
qCRH-R	CACTTCCCGATGATCTCCAT		
qSOD3-F	CTTTGTTCGGCCCGTACTCC	60	85
qSOD3-R	GCCTTGTTGTTGCCCTTGC		
qMYL9-F	CGTGCCAAAGCCAAGACCA	60	215
qMYL9-R	CTCGCTCATCATGCCTTCCAG		
qFOS-F	CTGGGTATCTCCAACTCGTATC	60	226
qFOS-R	GAACATTCAGACCACCTCAACA		
qRPIA-F	CACGCTGTGCATCGATTAGC	60	116
qRPIA-R	TCACTCAGCGTTAAGCCGTT		
qPGAM5-F	TGTCTGTCATGCCAACGTGA	60	215
qPGAM5-R	CTGGGTAGCCAGCTGTTTCA		
qIDH1-85-F*	AGAAGCAGGAGGAGGAGG	60	278
qIDH1-85-R	GATGCTCAATGCCCAAGT		
qIDH1-F	CATCCCTCGGTTGGTGTCT	60	144
qIDH1-R	GGTTTGCCTCCATCTCCTG		
qREEP5-41-F**	ATGCTCCCCATCTCCGTG	60	96
qREEP5-41-R	GCCGTAGCCGAACACCAG		
qREEP5-F	TTCCTGTCCTGGTTCCCTT	60	89
qREEP5-R	AACTCCGCTCCATTAGACG		

573 * qIDH1-85 represents the primers for XM_027461485.1 from *IDH1*.

574 ** qREEP5-41 represents the primers for XM_027446641.1 from *REEP5*.

575

bioRxiv preprint doi: https://doi.org/10.1101/2021.05.13.444049; this version posted May 14, 2021. The copyright holder for this preprint (which was not certified by peer review) is the author/funder, who has granted bioRxiv a license to display the preprint in perpetuity. It is made available under aCC-BY-NC-ND 4.0 International license.

576 **Table 2** The mapping statistics of validated reads

Sample	Valid reads	Mapped reads	Unique Mapped reads	Multi Mapped reads	PE Mapped reads*
C_H_1	51,239,468	40,246,810 (78.55%)	24,833,973 (48.47%)	15,412,837 (30.08%)	36,792,364 (71.80%)
C_H_2	49,409,120	41,287,364 (83.56%)	25,871,503 (52.36%)	15,415,861 (31.20%)	37,879,750 (76.67%)
C_H_3	50,247,476	42,241,544 (84.07%)	27,865,386 (55.46%)	14,376,158 (28.61%)	39,415,290 (78.44%)
C_H_4	38,820,220	29,069,218 (74.88%)	18,754,343 (48.31%)	10,314,875 (26.57%)	27,115,634 (69.85%)
C_P_1	49,967,938	42,615,294 (85.29%)	28,857,361 (57.75%)	13,757,933 (27.53%)	37,559,766 (75.17%)
C_P_2	49,527,692	42,214,709 (85.23%)	28,975,999 (58.50%)	13,238,710 (26.73%)	38,928,918 (78.60%)
C_P_3	53,769,752	45,507,234 (84.63%)	29,933,466 (55.67%)	15,573,768 (28.96%)	42,194,448 (78.47%)
C_P_4	42,013,858	34,274,240 (81.58%)	23,194,557 (55.21%)	11,079,683 (26.37%)	29,267,150 (69.66%)
FW_H_1	35,886,424	29,246,181 (81.50%)	19,000,230 (52.95%)	10,245,951 (28.55%)	27,082,722 (75.47%)
FW_H_2	45,611,570	38,161,438 (83.67%)	23,845,877 (52.28%)	14,315,561 (31.39%)	34,925,216 (76.57%)
FW_H_3	52,023,140	43,919,303 (84.42%)	28,939,721 (55.63%)	14,979,582 (28.79%)	40,876,986 (78.57%)
FW_H_4	52,987,882	44,676,116 (84.31%)	29,256,264 (55.21%)	15,419,852 (29.10%)	41,413,402 (78.16%)
FW_P_1	45,028,788	37,864,792 (84.09%)	25,480,801 (56.59%)	12,383,991 (27.50%)	34,984,564 (77.69%)
FW_P_2	51,144,142	42,671,489 (83.43%)	29,669,953 (58.01%)	13,001,536 (25.42%)	39,012,590 (76.28%)

bioRxiv preprint doi: https://doi.org/10.1101/2021.05.13.444049; this version posted May 14, 2021. The copyright holder for this preprint (which was not certified by peer review) is the author/funder, who has granted bioRxiv a license to display the preprint in perpetuity. It is made available under aCC-BY-NC-ND 4.0 International license.

FW_P_3	51,996,106	43,673,814 (83.99%)	28,161,497 (54.16%)	15,512,317 (29.83%)	40,726,292 (78.33%)
FW_P_4	50,619,482	39,540,336 (78.11%)	26,987,899 (53.32%)	12,552,437 (24.80%)	35,694,488 (70.52%)

577 * "PE Mapped reads" represents the pair-end mapped reads.

578

bioRxiv preprint doi: https://doi.org/10.1101/2021.05.13.444049; this version posted May 14, 2021. The copyright holder for this preprint (which was not certified by peer review) is the author/funder, who has granted bioRxiv a license to display the preprint in perpetuity. It is made available under aCC-BY-NC-ND 4.0 International license.

579 **Table 3** The significantly enriched pathways and enriched genes in the C_H vs.

580 FW_H.

Pathway name	p-value	Gene names
ECM-receptor interaction	0.000	*COL6A2, LAMA2, COL1A2, ITGB6, CHAD, COL4A4, COL4A3, SDC1, ITGB4, COL4A5, LAMB1, LAMA5*
Neuroactive ligand-receptor interaction	0.000	*LEPR, GH1, CGA, PRLHR, PRL, FSHB, TMEM139, NPBWR2, OXTR, MTNR1A, GAL, AVPR1B, GHRHR, TRHR, P2RX7, RXFP1, UCN3*
Focal adhesion	0.001	*COL6A2, LAMA2, COL1A2, ITGB6, CHAD, COL4A4, COL4A3, ITGB4, MYL9, COL4A5, LAMB1, LAMA5, PDGFRL*
Long-term depression	0.006	*CRH, LOC113845734*
Cytokine-cytokine receptor interaction	0.012	*LEPR, GH1, CSF3R, CXCL12, IL17RA, PRL, IL31RA, TNFRSF6B, CXCR6, IL18*
Regulation of actin cytoskeleton	0.024	*FGF19, IQGAP2, CXCL12, EZR, ITGB6, ITGB4, IQGAP3, MYL9, FGFR4*
Alcoholism	0.040	*ISLR, CRH, LOC113845734*
Cushing syndrome	0.042	*CRH, LOC113845734*
cGMP - PKG signaling pathway	0.048	*MYL9, RGS2*

581

bioRxiv preprint doi: https://doi.org/10.1101/2021.05.13.444049; this version posted May 14, 2021. The copyright holder for this preprint (which was not certified by peer review) is the author/funder, who has granted bioRxiv a license to display the preprint in perpetuity. It is made available under aCC-BY-NC-ND 4.0 International license.

582

583 **Table 4** The top 5 enriched KEGG pathways and enriched genes in C_P vs. FW_P

Pathway name	p-value	Gene names
ECM-receptor interaction	0.000	*COL6A1, CHAD, THBS2, SDC1, IBSP, TNR, SLITRK1, VWF, LAMA4, TNC, ITGA11, GP1BA, COL2A1*
Focal adhesion	0.001	*COL6A1, CAV3, CHAD, THBS2, IBSP, TNR, MYL9, VWF, PGF, LAMA4, TNC, ITGA11, COL2A1*
Neuroactive ligand-receptor interaction	0.001	*DRD5, GRM4, GPR50, CHRNA6, GLP1R, GRIA3, SSTR1, NMUR1, KBP, GRIN2C, VIP, CRAMP1, MLNR, MTNR1B*
Pantothenate and CoA biosynthesis	0.049	*PANK4, PANK3*
Vascular smooth muscle contraction	0.049	*ACTA2, CALCB, MYL9, KCNMB1*

584